Isothermal Crystallization and Chain Mobility of Poly(L-lactide)

S. IANNACE, L. NICOLAIS

Institute of Composite Material Technology (C.N.R.) and Department of Materials and Production Engineering, University of Naples "Federico II," P.le Tecchio 80, 80125, Naples, Italy

Received 16 February 1996; accepted 10 October 1996

ABSTRACT: Isothermal melt crystallization of poly(L-lactide) (PLLA) has been studied in the temperature range of 90 to 135°C. A maximum in crystallization kinetic was observed around 105°C. A transition from regime II to regime III is present around 115°C. The crystal morphology is a function of the degree of undercooling. At crystallization temperatures (T_c) below 105°C, further crystallization occurs upon heating; this behavior is not detected for T_c above 110°C. The analysis of the heat capacity increment at glass transition temperature (T_g) and of dielectric properties of PLLA indicates the presence of a fraction of the amorphous phase which does not relax at the T_g, and the amount of this so-called rigid amorphous phase is a function of T_c. © 1997 John Wiley & Sons, Inc. J Appl Polym Sci **64:** 911–919, 1997

Key words: poly(L-lactide); regime transition; crystallization kinetics; rigid amorphous fraction

INTRODUCTION

Poly(L-lactide) (PLLA) is a biodegradable polymer widely studied either for biomedical applications[1] or to replace commodity polymers in packaging and other fields where the degradation of the material is an important prerequisite for environmental reasons.[1–5]

Studies regarding the morphology and crystal growth of PLLA as a function of molecular weight and crystallization temperature (T_c) from the melt, has been reported in literature.[6] The samples with higher molecular weight showed spherulitic morphology following a regime II of crystallization. According to the theory proposed by Hoffman and associates,[7] this implies that lateral crystal growth is slow compared with the number of crystal nuclei. Above 163°C the polymer showed a transition to a regime I of crystallization, which corresponds to axialite formation. However, no information was available at temperatures below 114°C due to high nucleation density which did not allow a clear detection of the crystal growth.

The study of the crystallization phenomena is of great importance in polymer processing, for several reasons. The control of the temperature profile during cooling, in the final stage of a process, determines the development of a specific morphology which influences the final properties of the material. Cooling rate is therefore important and it can be adjusted to modulate the level of crystallinity and the crystal morphology of a polymer. However, the modeling of nonisothermal crystallization implies the knowledge and modeling of isothermal phenomena which give information on kinetics and morphology developed at each crystallization temperature.[8–10] Since T_c is among the factors determining the thermodynamics and kinetics of structure formation, a great variety of morphologies and supermolecular formations can be obtained by changing the degree of undercooling during the crystallization process of flexible chain polymers.[11–13]

Correspondence to: S. Iannace.

The structure and the molecular mobility of the amorphous phase, which develops in semicrystalline polymers, are strongly affected by the crystal morphology and have been the focus of an increasing number of studies in recent years. If crystallization is performed at high undercooling, the molecular mobility is reduced and the crystal growth rate is lower compared with the nucleation rate. As a consequence, an elevated number of small crystals will develop, which results in a high amount of interconnected chains between the crystals that were not able to be adsorbed in the lamellar thickness. These tie chains have lower mobility compared with the bulk of the amorphous phase, and do not necessarily assume liquidlike mobility above the glass transition temperature (T_g). The presence of amorphous immobilized chain segments was recognized in several crystalline polymers [i.e., polyethylene terephthalate (PET)[14] β-propiolactone,[15] and poly(oxymethylene)[16]] and quantitative analysis of this so-called rigid amorphous fraction can be achieved by measuring the variation of the heat capacity (C_p) around the T_g through the following expressions[17,18]:

$$X_{\text{raf}} = fr - X_c \tag{1}$$

$$fr = 1 - \left[\frac{\Delta C_p(c)}{\Delta C_p(a)}\right] \tag{2}$$

where fr is the overal "rigid fraction," X_c is the crystallinity measured from the heat of fusion of the crystallized samples, and $\Delta C_p(c)$ and $\Delta C_p(a)$ are the measured heat capacity increase at the T_g, respectively, for crystalline and amorphous samples.

In this work isothermal melt crystallization of PLLA has been studied in the temperature range of 90–135°C. Melting behavior and molecular mobility of the amorphous phase were analyzed as functions of crystallization temperature by performing calorimetric and dielectric experiments.

MATERIALS AND METHODS

PLLA (Resomer™ L214 from Boehringer Ingelheim, Germany) was isothermally crystallized in the temperature range of 90 to 135°C by means of a Mettler differential scanning calorimeter. The samples were first melted for 2 min at 200°C, then cooled to the crystallization temperature for 30 min to allow complete crystallization. Because of the relatively slow crystallization during cooling from melt, we were able to follow the evolution of crystallinity at relatively low T_c on amorphous samples which did not crystallize during cooling. Crystallization kinetic was evaluated calculating the relative crystallinity $X_r(t)$ at time t as the fractional area confined between the heat flow-time curve and the baseline of the isothermal calorimetric curves. In the temperature range investigated, the crystallization was slow enough to be followed accurately.

A second scan from 10°C to 220°C was then performed on all the isothermally crystallized samples with a heating rate of 10°C/min. The presence of the so-called rigid amorphous fraction (X_{raf}) was evaluated by measuring the heat capacity increase at the T_g according to eqs. (1) and (2).[17–19] $\Delta C_p(c)$ and $\Delta C_p(a)$ at $T = T_g$ in eq. (2) were calculated by a linear extrapolation of the liquid heat capacity above T_g and from solid heat capacity below T_g.

The degree of crystallinity (X_c) was measured from the isothermal heat of crystallization (ΔH_c) at the completion of crystallization as follows:

$$X_c = \frac{\Delta H_c}{81} \tag{3}$$

where 81 J/g was used as the heat of fusion of the crystalline phase of PLLA.[4,20]

Dielectric measurements were performed on thin films (50–100 μm) using a Dielectric analyzer DEA 2970 (TA Instruments, Coventry, UK). All films were first prepared by casting from a solution of chloroform; after the evaporation of solvent, they were isothermally crystallized by a Mettler hot stage. As for differential scanning calorimetry (DSC) analysis, melt crystallization was achieved by the following procedures: (a) melting at 200°C for 2 min to destroy crystallinity; (b) quick cooling to the crystallization temperature; and (c) isothermal for 30 min.

RESULTS AND DISCUSSION

Melt Crystallization Kinetics

Isothermal experiments performed on PLLA are reported in Figure 1. The symmetrical shape of the exothermic crystallization peak, shown in Figure 1(a), suggests that the crystallization process does not present any secondary crystallization,

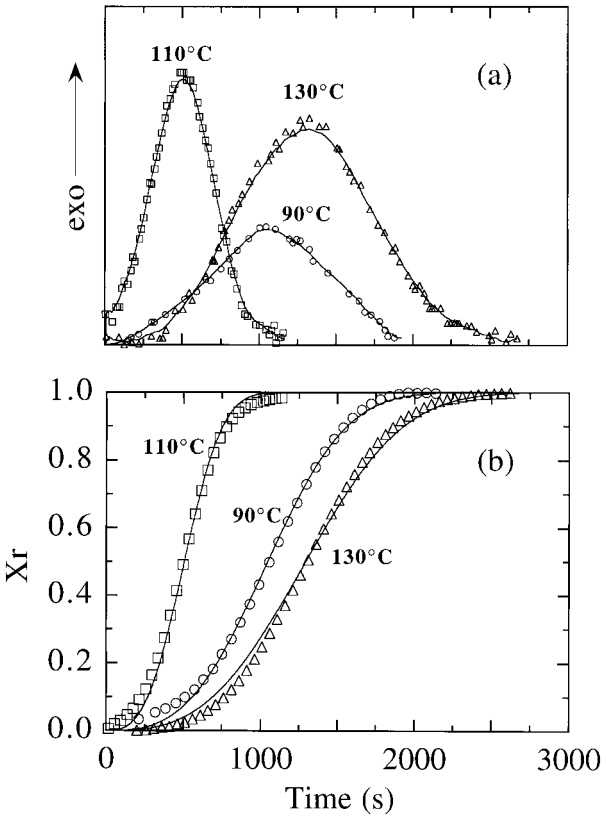

Figure 1 Isothermal melt crystallization at T_c indicated. Heat flow (a) and relative crystallinity (b) versus crystallization time.

which is usually accompanied by a long term of heat flow beyond the exothermic maximum.[12,21,22]

The theory of Avrami[23] was used to analyze the increase of the relative crystallinity with time [Fig. 1(b)]:

$$X_r(t) = 1 - \exp(-Kt^n) \quad (4)$$

where the values of K and n, which are considered to be diagnostic to the mechanism of crystallization,[24] are respectively related to the crystallization half-time and to the type of nucleation together with the geometry of the crystal growth. Avrami constants K and n for PLLA are summarized in Table I. They were calculated by plotting $\log[-\ln(1 - X_r)]$ versus $\log(t)$ and evaluating the slope, the Avrami exponent n, and the intercept, the constant $\log(K)$.

Preliminary analysis[19] showed that a single Avrami exponent can describe the melt crystallization of PLLA from a certain value of crystallinity (~0.03) until its completion, and therefore a single mechanism governs the entire process at each value of crystallization temperature T_c. As listed in Table I, the value of n close to 3, for all the T_c investigated, is an indication that the growing of crystals is three-dimensional and athermal. The lower values of n observed in few cases can be related to the presence of crystals that were not completely melted at 200°C and/or to the formation of a small, ordered structure, developed during cooling, which acted as crystal seed nuclei. The increase of n for $T_c > 125$°C is an indication that the growing mechanism is changing; it becomes intermediate between the athermal ($n = 3$) and thermal ($n = 4$) types of nucleation.[25]

Analysis of the half-time values (Table I) indicates that the time taken for half of the crystallization to develop is a strong function of T_c. Using a theoretical approach, it can be shown that the linear growth rate G can be considered proportional to $1/t_{1/2}$ and, based on the Hoffman–Lauritzen theory,[7,9,26] the temperature variation of $1/t_{1/2}$ can be written as:

$$\left(\frac{1}{t_{1/2}}\right) = \left(\frac{1}{t_{1/2}}\right)_0 \exp\left[-\frac{U}{R(T_c - T_\infty)}\right] \times \exp\left[-\frac{K_g}{T_c \Delta T f}\right] \quad (5)$$

In this equation, the first exponential controls the rate variations occurring at high degree of undercooling where the overall crystallization is dominated by the chain mobility, which decreases when the temperatures approach the material's T_g. U is the activation energy for segmental jump rate in polymers; $T_\infty = T_g - 30$ K; and R is the universal gas constant. For temperatures close to

Table I Avrami Parameters and Crystallization Time ($t_{1/2}$) Calculated at $X_r = 0.5$

T_c (°C)	n	$\log[K(s^{-n})]$	$t_{1/2}$ (s)
90	2.91	−8.95	1,066
95	2.85	−7.89	519
100	2.80	−7.45	392
105	2.85	−7.31	325
110	2.76	−7.61	502
115	3.09	−8.96	717
120	2.87	−8.44	764
125	3.06	−9.10	821
130	3.23	−9.28	1,071

T_∞, the exponential tends to zero because the mobility of chains is remarkably reduced.

The second exponential accounts for the driving force of crystallization and contains thermodynamic characteristics such as heat of fusion, side and fold surface free energy, and the infinite-crystal melting point T_m^0. The functionality of this term from the degree of undercooling ($\Delta T = T_m^0 - T_c$), which constitutes the driving force of crystallization, indicates that the substantial meaning of the term is to account for the decrease in the overall rate when temperature approaches the thermodynamic melting point. The correction term $f = 2T_c/(T_c + T_m^0)$ is introduced to account for changes in heat of fusion with the crystallization temperature T_c. Constant K_g contains a constant n whose value depends upon the crystallization regime.[27]

In order to verify the crystallization regimes in the temperature range investigated, we have plotted $\ln(1/t_{1/2}) + U/R(T_c - T_\infty)$ versus $1/T_c\Delta Tf$ (Fig. 2). Several values of U were selected for analysis of the results. The thermodynamic melting temperature T_m^0, evaluated by a Hoffmann–Weeks analysis (see below), was equal to 479 K. The presence of two regions with different slopes is an indication that a transition from regime II to regime III occurs around 115°C, and this behavior was observed for all the values given to the activation energy.

U = 1,500 cal/mol, utilized in a previous study on PLLA,[6] was employed here to fit the experimental data below T_c = 115°C and a value of $K_{g(\mathrm{III})} = 8.91 \cdot 10^5$ was obtained. The theoretical curve is reported in Figure 3 (curve III) together with the experimental data. Similar calculations were performed on the $1/t_{1/2}$ data above 115°C. The best fitting is in this case was obtained with U = 1,500 and $K_{g(\mathrm{II})} = 2.92 \cdot 10^5$. The nucleation constant $K_{g(\mathrm{II})}$ in regime II is in agreement with the results reported in literature,[6] but the value of $K_{g(\mathrm{III})}$ is higher than the value predicted by the theory. The slope ratio $K_{g(\mathrm{III})}/K_{g(\mathrm{II})}$ is 3.05, and it is higher than the theoretical value 2. This could be related to the wrong set of values utilized for U, T_∞. These values are very close to those reported by Vasanthakumari and Penning[6] but they seems to be not appropriate for our experimental data.

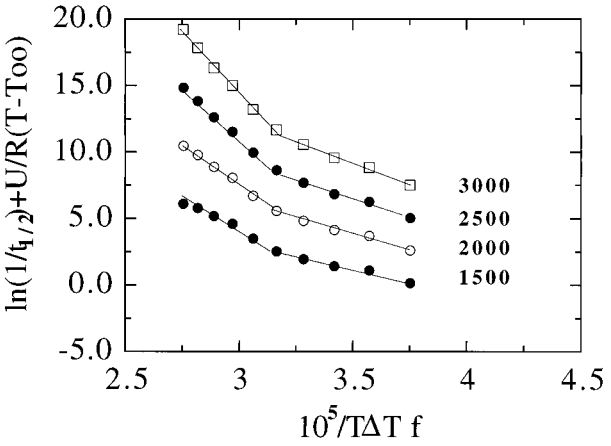

Figure 2 Kinetic analysis of the growth rate data for PLLA, using different values of U (cal/mol). T_m^ϕ = 206.2°C, T_g = 62.5°C, $T_\infty = T_g - 30$°C.

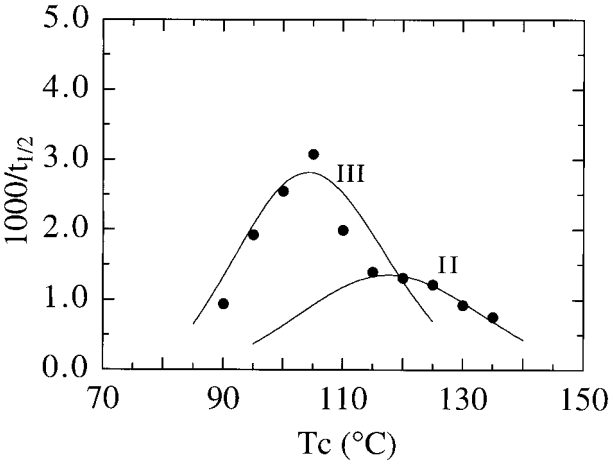

Figure 3 Comparison between experimental data and calculation (solid line) of the half-times as functions of the crystallization temperature.

Melting Behavior

Figure 4 reports the DSC scans after the isothermal crystallization. The curves show a progressive melting for T_c ranging from 110 to 135°C [Fig. 4(b)] whereas for crystallization temperatures lower then 105°C [Fig. 4(a)] we observed the presence of a small exothermal phenomena before the endothermal melting. A possible explanation of this behavior is that in this temperature range, where we observed a regime III of crystallization, nucleation rate and crystal growth are much higher than the time requested for chain disentanglement. Then, either the degree of perfection of the crystals or the maximum crystallinity achievable is therefore affected by the restricted mobility of the chains, which does not allow the growth of well-developed lamellar crystals. The increase in the molecular mobility, gained by the increase in temperature, may result in a further

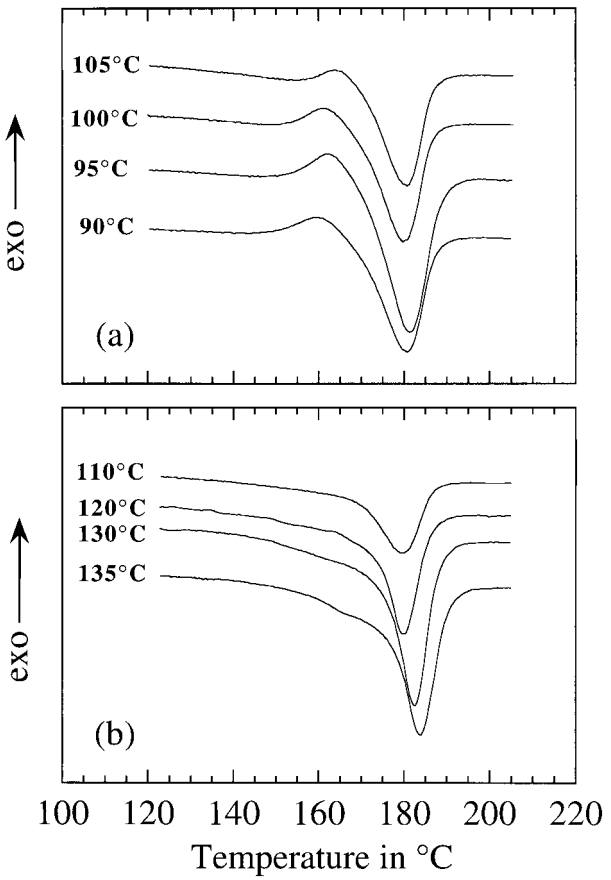

Figure 4 DSC scans at 10°C/min, showing the effect of the crystallization temperature.

crystallization just before the melting of the formed crystals. Measurements carried out at different heating rates would clarify the presence of recrystallization/reorganization phenomena that occur upon heating. This behavior has been observed for other thermoplastic polymers such as poly(thio-1,4-phenylene) (PPS)[28,29,30] and poly(aryl ether ether ketone) (PEEK)[21,31] but this analysis would be beyond the purpose of this work.

The Hoffmann–Weeks plot of the DSC data are reported in Figure 5. Only data above 110°C were utilized for a linear regression of the crystallization data, and a good alignment on the straight line was confirmed by the correlation coefficient $R = 0.993$. Extrapolation of the experimental results gives a thermodynamic melting point of 206.2°C which, in spite of the few data available, appears to be very close to that reported in literature.[6]

When the high-molecular-weight PLLA is crystallized in the range of 90 to 105°C, a large number of molecular chains become part of several nuclei; this results in the hindering of the molecular mobility, which contributes to reducing the degree of crystallinity. This is confirmed by the analysis of X_c versus T_c reported in Figure 6. The slope variation, occurring between 110 and 120°C, is again related to the regime transition previously discussed.

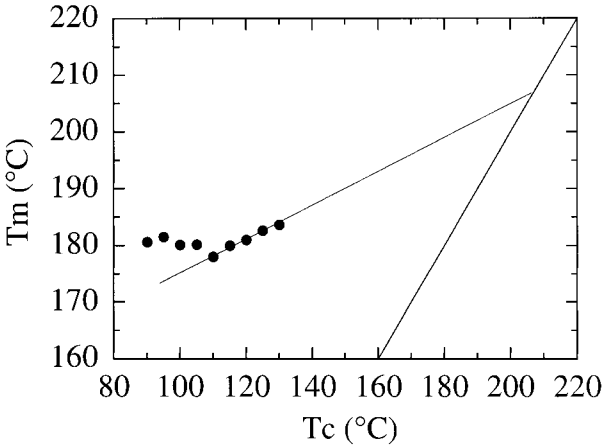

Figure 5 Hoffman–Weeks analysis. Melting point T_m as a function of the crystallization temperature.

As a consequence of the different crystallization conditions, different morphologies were obtained by varying the level of undercooling. Higher numbers of nuclei were formed at lower T_c, which led to the formation of higher numbers of crystals with smaller sizes.[19]

The Amorphous Domain

T_gs of the isothermally crystallized samples, measured at the inflection point of the calorimetric

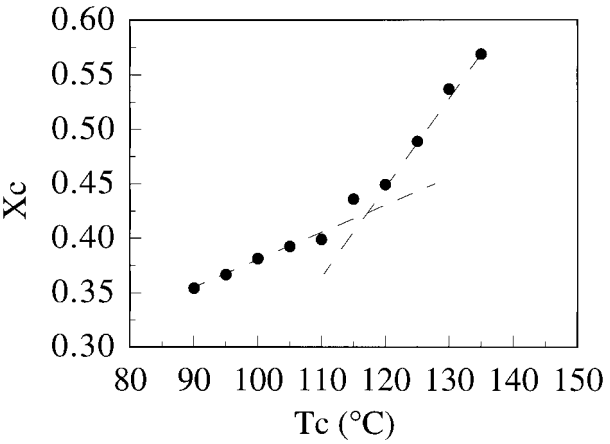

Figure 6 Degree of crystallinity X_c versus T_c.

Table II T_g, Total Rigid Fraction (fr), Rigid Amorphous Fraction (X_{raf}), and Activation Energy as Function of T_c

T_c (°C)	T_g (°C)	X_c	fr	X_{raf}	ΔE (cal/mol)
90	70.9	0.35	0.64	0.29	115.8
95	70.0	0.37	0.69	0.32	116.8
100	69.1	0.38	0.63	0.25	116.9
105	68.3	0.39	0.66	0.27	114.3
110	68.1	0.40	0.64	0.24	108.2
115	67.9	0.43	0.60	0.17	102.5
120	67.5	0.45	0.56	0.11	101.6
125	67.3	0.49	0.58	0.09	95.6
130	67.2	0.54	0.57	0.03	93.4
135	67.3	0.57	0.58	0.01	93.3

curve, are reported in Table II. Variation from 71°C, observed for T_c = 90°C, to about 67°C for T_c = 130°C is the first indication that the mobility of the amorphous region is sensitively reduced in samples crystallized at high degrees of undercooling. The decrease in mobility cannot be related to variations in the degree of crystallinity because we should have observed an increase of T_g versus T_c. The specific crystalline phase and morphology developed at T_c impose constraints on the amorphous phase, reducing the available configurations of the molecular chains. As expected, the maximum mobility was observed in totally amorphous samples that showed a T_g of 62.5°C.

Further investigations were carried out on the calorimetric results in order to achieve more information about the relaxation process which takes place at T_g. The analysis of the increment of heat capacity $C_p(T)$ was therefore performed, since it is directly related to the fraction of amorphous material relaxing at T_g. The variation in the heat capacity is considered to come only from the mobile amorphous fraction, which becomes liquid within a narrow range of temperature around T_g. The difference between the liquidlike fraction and the rigid part of the amorphous phase is related to the different configurational entropy of the chains; this results in the absence of a distinct heat-capacity change at the glass transition step, where we observed only the transition of the most mobile amorphous fraction. Comparing the heat capacity increment of semicrystalline and quenched amorphous materials at T_g, as specified in eqs. (1) and (2), it was consequently possible to evaluate the fraction of amorphous molecules that do not become liquidlike at T_g. The results of the examination are shown in Figure 7 and the relative data are reported in Table II. The small variations of the total rigid fraction $fr = X_{raf} + X_c$ indicates that the amount of molecules not relaxing at T_g reduced just 10% when the crystallization temperature increased from 90°C to 130°C. Because of the crystallinity increases of more than 50% in the same range of temperature, it follows that a significant variation occurs in the rigid amorphous fraction X_{raf}. Moreover, correspondence between slope variation of X_{raf} versus T_c (Fig. 7) and regime transition indicates that these two phenomena are related.

The debate on the dependence of X_{raf} from the intrinsic stiffness of the polymer chain and the crystal morphology controlled by the crystallization kinetics is still open.[22] The portion of amorphous phase which does not gain liquidlike mobility at the glass transition was, however, recognized for several engineering polymers such as poly(oxymethylene) and poly(oxyethylene),[16] PET,[14] Poly(α-dialkyl-β-propiolactones),[15] PPS,

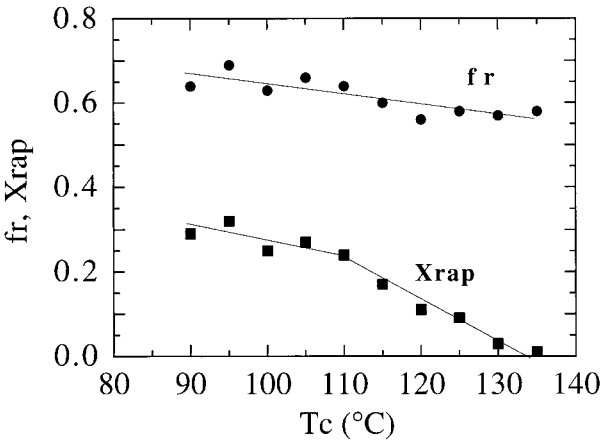

Figure 7 Total rigid fraction (●) and rigid amorphous fraction (■) as function of T_c.

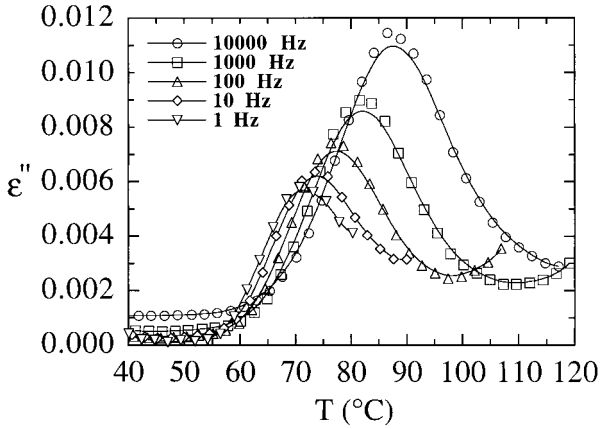

Figure 8 Imaginary part of the dielectric function (ε'') as function of frequency, melt-crystallized at 100°C.

and PEEK.[17,18] It has been shown that a very large weight fraction of rigid amorphous material was obtained for cold crystallized samples, larger than that arising from either melt crystallization or slow cooling treatments.

The interconnection of amorphous and crystalline phases has profound and interesting effects on the relaxation behavior and the mechanical properties of a polymer. One consequence of the existence of a fraction of reduced mobility in the amorphous phase is that the two-phase model of well-developed crystals plus the amorphous fraction may be inadequate to explain the modulus variation with crystallinity[32] and therefore more complex models have to be developed to predict the behavior of the material. Analogous problems such as the physical aging of polymers can be expected from viscoelastic and viscoelastic-related studies, due to the strong dependence of these problems on the molecular mobility and its distribution in the amorphous phase.

Dielectric Analysis

Dielectric relaxation is a useful tool to examine the molecular mobility of polymeric chains. In order to investigate a wide range of this behavior, the analysis was performed varying both frequency and temperature. The approach is based on the assumptions that dipole relaxation depends upon the local environment and that the response to an applied electric field is associated to local mobility. At a certain frequency and temperature, the amount of dipoles that can respond to the electric field is therefore related to their ability to move. As an example, crystalline dipoles are more tightly bound in the environment than amorphous dipoles, and thus they are not able to respond at certain frequency. Equivalently, dipoles that are part of the rigid amorphous phase have lower mobility and respond differently than the "liquidlike" amorphous molecules.

The temperature dependence of dielectric loss ε'', at various frequencies in the glass transition region, is reported in Figure 8. As expected, ε'' shows a well-defined peak at each frequency, whose intensity increases and shifts to higher temperature as the applied frequency increases. The analysis of the chain stiffness against the segment motions was performed by calculating the apparent energy of activation (ΔE) of the relaxation process by means of the following Arrhenius equation:

$$f = f_0 \exp\left(-\frac{\Delta E}{RT}\right) \tag{6}$$

where f is the applied frequency, T is the temperature corresponding to the maximum values of ε'', and f_o is the extrapolation of the frequency at $T = \infty$. A representation of this behavior is reported in Figure 9, where the experimental data are aligned on a straight line. The activation energy, calculated from the above slopes, are reported in Table II and shown in Figure 10 versus the crystallization temperature T_c.

The decrease of ΔE is in agreement with the above results obtained from thermal analysis. The rigid amorphous fraction X_{raf} and the apparent activation energy show similar trends. Little vari-

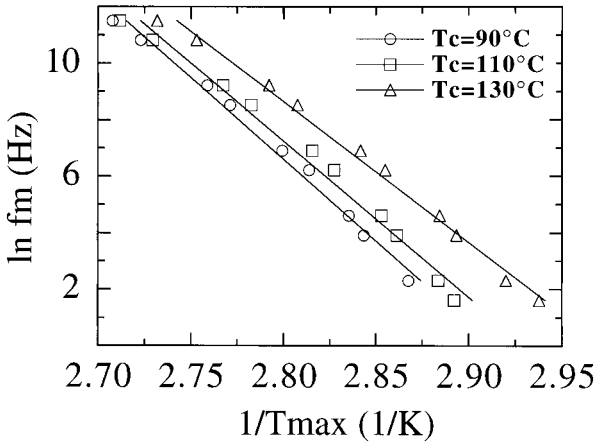

Figure 9 Arrhenius plot of the frequency of the ε'' maximum.

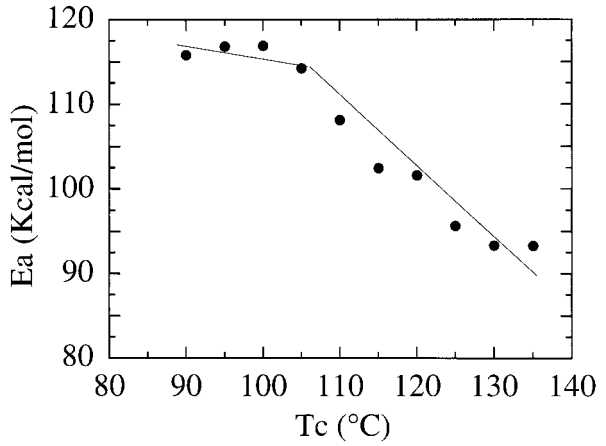

Figure 10 Activation energy as function of the crystallization temperature.

ation was observed for T_c up to 105°C, followed by a progressive reduction of the immobilization effect in the amorphous phase. This is accompanied by a contemporary decrease of the apparent activation energy ΔE, which can be seen as the thermodynamic barrier to the molecular movement.[33]

In stress relaxation experiments the apparent activation energy is a measure of the chain stiffness against segment motion. At the T_g, the long-range movements become predominant, if compared with the short-range molecular motions occurring below T_g,[34,35] and ΔE is related to the energy required for this type of movement. The activation energy of the dielectric relaxation has an analogous meaning, even though it is the result of different types of experiments. The increasing values of ΔE, observed at lower crystallization temperatures, indicate that the required energy for the movements of the amorphous chains is a growing function of the degree of undercooling.

CONCLUSIONS

Isothermal crystallization kinetics of PLLA were studied as a function of the degree of undercooling. The overall rate of bulk crystallization follows an Avrami equation with the exponent n close to 3. The crystallization rate shows a maximum around 105°C.

Regime analysis allowed the detection of a II → III transition around 115°C. For value of the activation energy U = 1,500 cal/mol, the regime III/II slope ratio is 3, which is higher than the theoretical value 2.

When PLLA is crystallized at high undercooling, crystallization is not complete and exothermal crystallization occurs at temperatures close to the melting point of the already-formed crystals.

Analysis of the heat capacity increment at T_g of semicrystalline PLLA indicates the presence of an amorphous fraction which does not relax at T_g. Higher amounts of this rigid–amorphous phase were observed for $T < 110$°C. Lower and decreasing values were detected for T_c above 110°C, where regime transition occurs. Analysis of the activation energy of the relaxation behavior, performed by dielectric experiments, confirms the variation of the molecular mobility of the amorphous phase with T_c.

The authors thank Mr. G. Bruno for his help in performing most of the calorimetric experiments, and particularly acknowledge Dr. A. D'Amore for helpful discussions.

REFERENCES

1. M. Vert, S. M. Li, G. Spenlehauer, and P. Guerin, *J. Mat. Sci.: Materials in Medicine,* **3,** 432 (1992).
2. S. Gogoleski, *Clin. Mater.,* **10,** 13 (1992).
3. M. Vert, G. Schwarch, and J. Coudane, *J. Macr. Sci.-Pure Appl. Chem.,* **A32**(4), 787 (1995).
4. S. Iannace, L. Ambrosio, S. J. Huang, and L. Nicolais, *J. Appl. Polym. Sci.,* **54,** 1525 (1994).
5. S. Iannace, L. Ambrosio, S. J. Huang, and N. Nicolais, *J. Macr. Sci.-Pure Appl. Chem.,* **A32**(4), 881 (1995).
6. R. Vasanthakumari and A. J. Pennings, *Polymer,* **24,** 175 (1983).
7. J. D. Hoffman, L. J. Frolen, G. S. Ross, and J. I. Lauritzen, Jr., *Journal of Research of the National Bureau of Standards-A. Physics and Chemistry,* **79A,** 671 (1975).
8. A. Maffezzoli, J. M. Kenny, and L. Nicolais, *J. Mat. Sci.,* **28,** 4994 (1993).
9. R. M. Patel and J. E. Spruiell, *Polym. Eng. Sci.,* **31,** 730 (1991).
10. D. J. Blundell and B. N. Osborn, *SAMPE Quarterly,* **17,** 1 (1985).
11. P. J. Lemstra, J. Postma, and G. Challa, *Polymer,* **15,** 757 (1974).
12. P. C. Vilanova, S. M. Ribas, and G. M. Guzman, *Polymer,* **26,** 423 (1985).
13. G. K. Elyashevich and V. I. Poddubny, *J. Macromol. Sci., Phys.,* **B29,** 249 (1990).

14. J. C. Coburn and R. H. Boyd, *Macromolecules,* **19,** 2238 (1986).
15. R. Plesu, T. M. Malik, and R. E. Prud'homme, *Polymer,* **33,** 4463 (1992).
16. H. Suzuki, J. Grebowicz, and B. Wunderlich, *Makromol. Chem.,* **186,** 1109 (1985).
17. S. Z. D. Cheng, S. Lim, L. H. Judovits, and B. Wunderlich, *Polymer,* **28,** 10 (1987).
18. S. Z. D. Cheng, Z. Q. Wu, and B. Wunderlich, *Macromolecules,* **20,** 2802 (1987).
19. S. Iannace, L. Ambrosio, and L. Nicolais, in *Proc. 1st Symposium on "Frontiers in Biomedical Polymers,"* June 1995, Santa Margherita Ligure (Portofino, Riviera Ligure), Italy.
20. E. W. Fisher, H. J. Sterzel, and G. Wegner, *Kolloid-Z.u.Z. Polim.,* **251,** 980 (1973).
21. P. Cebe and S. D. Hong, *Polymer,* **27,** 1183 (1986).
22. P. P. Huo, J. B. Friler, and P. Cebe, *Polymer,* **34,** 4387 (1993).
23. M. Avrami, *J. Chem. Phys.,* **8,** 212 (1940).
24. D. W. Van Krevelen, *Properties of Polymers,* Elsevier, New York, 1990.
25. B. Wunderlich, *Macromolecular Physics,* Academic Press, New York, 1976.
26. J. D. Hoffman, G. T. Davis, and J. I. Lauritzen, *Treatise on Solid State Chemistry: Crystalline and Non-crystalline Solids,* Plenum, New York, 1976.
27. J. D. Hoffman, *Polymer,* **24,** 3 (1983).
28. A. J. Lovinger, D. D. Davis, and F. J. Padden, *Polymer,* **26,** 1595 (1985).
29. J. S. Chung and P. Cebe, *Polymer,* **33,** 2312 (1992).
30. J. S. Chung and P. Cebe, *Polymer,* **33,** 2325 (1992).
31. D. J. Blundell, *Polymer,* **28,** 2248 (1987).
32. R. Boyd, *Polymer,* **26,** 323 (1985).
33. N. G. McGrum, B. E. Read, and G. Williams, *Anelastic and Dielectric Effects in Polymeric Solids,* John Wiley & Sons, New York, 1967.
34. J. Noah and R. E. Prud'homme, *Macromolecules,* **12,** 721 (1979).
35. J. Noah and R. E. Prud'homme, *Macromolecules,* **12,** 300 (1979).